J. Biochem. **136**, 839–846 (2004)
DOI: 10.1093/jb/mvh194

Incorporation of an Azobenzene Derivative into the Energy Transducing Site of Skeletal Muscle Myosin Results in Photo-Induced Conformational Changes

Nobuhisa Umeki[1,2], Tsuyoshi Yoshizawa[1], Yasunobu Sugimoto[3], Toshiaki Mitsui[2], Katsuzo Wakabayashi[3] and Shinsaku Maruta[1,*]

[1]Division of Bioengineering, Graduate School of Engineering, Soka University, Hachioji, Tokyo 192-8577; [2]Group of Plant and Microbial Genome Controls, Graduate School of Science and Technology, Niigata University, Niigata 950-21; and [3]Division of Biophysical Engineering, Graduate School of Engineering Science, Osaka University, Toyonaka, Osaka 560-8531

Received May 6, 2004; accepted October 15, 2004

The region containing reactive cysteines, Cys 707 (SH1)–Cys 697 (SH2), of skeletal muscle myosin is thought to play a key role in the conformational changes of the myosin head during force generation coupled to ATP hydrolysis. In the present study, we synthesized a photochromic crosslinker, 4,4′-azobenzene-dimaleimide (ABDM), that undergoes reversible *cis-trans* isomerization upon ultra violet (UV) and visible (VIS) light irradiation resulting in a change in the crosslinking length from 5 to 17 Å. The reactive cysteines, SH1 and SH2, of myosin subfragment 1 (S1) were crosslinked with ABDM, yielding an ABDM-S1 complex. The changes in absorbance induced by UV/VIS light irradiation of the complex were similar to those of free ABDM indicating that the incorporation of ABDM at the SH1 and SH2 sites did not disrupt the isomerization of crosslinked ABDM. Small-angle synchrotron X-ray scattering analysis of the ABDM-S1 complex in solution suggested that the localized conformational changes resulting from the *cis* to *trans* isomerization on ABDM crosslinking of SH1 and SH2 induced a small but significant swing in the lever arm portion of S1 in the opposite direction from that induced by ATP.

Key words: conformational change, crosslink, energy transduction, isomerization, myosin subfragment 1, photochromic molecule, X-ray small-angle scattering.

Abbreviations: ABDM, 4,4′-azobenzene-dimaleimide; AD, 6-acryloyl-2-dimethyl-aminonaphthalene; BD, 6-bromoacetyl-2-dimethyl-aminonaphthalene; DIAAB, 4,4′-diiodoacetamideazobenzene; FHS, 6-[fluorescein-5(and 6)-carboxyamido]hexanoic acid succinimidylester ; *p*PDM, *N,N′-p*-phenylenedimaleimide; S1, myosin subfragment-1. Enzymes: myosin ATPase [EC 3.6.1.32]; chymotrypsin [EC 3.4.21.1]; papain [EC 3.4.22.2].

Myosin is a motor protein that moves along actin filaments by using the energy generated on ATP hydrolysis. X-ray small-angle scattering (*1*, *2*), quick freeze deep etch replica electron microscopy (*3*), and biochemical experiments (*4*–*7*) have demonstrated that the lever arm portion of the myosin motor domain swings during ATP hydrolysis. The swinging motion of the lever arm of a myosin head may be directly related to the generation of motility force. However, the precise molecular mechanism underlying the energy transduction and how ATP hydrolysis causes the swinging motion of the lever arm have remained to be investigated. Recent X-ray crystallographic studies of myosin heads corresponding to several transient states in the myosin ATPase cycle (*8*–*14*) suggested that the chemical energy of ATP is mechanically transmitted for the physical swinging of the lever arm to occur like a cam-shaft motion through subdomain steric interactions. First, ATP binding to the catalytic site of S1 induces a conformational change of the switch II loop resulting in glycine (Gly) 457 of the loop forming a hydrogen bond with the γ-phosphate of ATP. The movement of Gly 457 makes the side chain of phenlyalanine (Phe) 458 rotate and strongly interact with the relay helix via hydrophobic forces. This change results in rotation of the relay helix, subsequently causing rotation of the converter domain to induce a lever arm swing.

Supporting this idea, disruption of the hydrophobic interaction between the relay helix and the converter domain in S1 by a point mutation uncouples the rotation of the converter domain from the hydrolysis cycle of ATP (*15*). It has also been shown that the steric interactions between the glycine residue located within the reactive cysteine (Cys) (SH1-SH2) region and the phenylalanine residue in the relay helix are essential for mediating communications between the nucleotide binding site and the converter domain (*16*).

It is well established that the reactivity of the sulfhydryl groups on Cys 707 (SH1) and Cys 697 (SH2) is very sensitive to nucleotide binding. Moreover, these two residues can be crosslinked by a variety of bifunctional reagents of different lengths (*17*–*19*), and in the swinging lever arm model, this flexible region has been identified as a fulcrum point (*20*). Based on the results of fluorecence intensity analysis of attached fluorescent probes, Hiratsuka (*21*) suggested that the SH1-SH2 region acts as an energy transduction loop through which intersite

*To whom correspondence should be addressed. Phone: +81-426-91-9443, Fax: +81-426-91-9312, E-mail: shinsaku@t.soka.ac.jp

communications between ATP and actin binding sites are transmitted.

Photochromic molecules, which can undergo a reversible configurational change upon light irradiation, have been applied for dimmer materials, optical storage materials, indicator materials and so on (*22–24*). Azobenzene, a widely studied photochromic compound, can be reversibly isomerized between the cis and trans forms by UV and VIS light irradiation, respectively (*25–26*). Interestingly, it has been shown that the *cis-trans* isomerization of an azobenzene derivative crosslinked to an α-helical synthetic peptide induces a reversible change in the secondary structure of the peptide from a helix to a random coil and vice versa on UV/VIS photoirradiation (*27–28*).

In the present study, the azobenzene derivative, 4,4′-azobenzene-dimaleimide (ABDM) was incorporated into the SH1-SH2 region of skeletal muscle myosin S1, which may be one of the energy transducing portions and was used as a mechanical energy input unit for a motility force. Myosin heads were modified with ABDM, and then whether or not the *cis-trans* isomerization of the crosslinked ABDM by UV/VIS light can induce a global conformational change of S1 was investigated. It is shown that the *cis-trans* isomerization of ABDM causes swinging of the lever arm of S1 in the opposite direction to that induced by ATP binding. This technique may contribute to the understanding of the energy transduction mechanism in a myosin molecule. Moreover, photochromic molecules such as azobenzene derivatives may be applicable to the study of other energy transducing proteins.

MATERIALS AND METHODS

Protein Preparation—Myosin was prepared from chicken breast muscle according to the procedure of Perry (*29*). To obtain subfragment 1 (S1), myosin molecules were digested with α-chymotrypsin as reported by Weeds and Taylor (*30*) or with papain according to the method of Margossian and Lowey (*31*). F-actin was prepared from chicken skeletal muscle as described by Pardee and Spudich (*32*).

Synthesis of 4,4′-Azobenzene-Dimaleimide (ABDM)—ABDM was prepared by coupling 4,4′-diazoaniline with two equivalents of maleic anhydride, and subsequent maleimide ring closure was performed by treatment with acetic anhydride using the modified procedure of Nishimura *et al.* (*33*). Maleic anhydride (472 μmol) and 4,4′-azoaniline (236 μmol) were added to 2.6 ml of tetrahydrofuran (THF) solution. The resulting mixture was stirred magnetically at 4°C for 24 h. The insoluble 4,4′-azobenzene maleic acid derivative was pelleted by centrifugation at low speed for 5 min. The supernatant was removed, and the precipitate was resuspended in 2.6 ml of THF solution. The mixture was centrifuged again, and the supernatant was discarded. The precipitate was suspended in 2.6 ml of THF solution in a vial, and then acetic anhydride (0.5 ml) and anhydrous sodium acetate (50 mg) were added to the solution. The vial was evacuated and sealed at –20°C. After warming to room temperature the vial was heated to 100°C for 22 h. The vial was cooled to 0°C and then opened. Distilled water (10 ml) was added to the vial, and then the mixture was stirred for 10 min at 4°C to precipitate the ABDM. The precipitate was collected by low speed centrifugation and dissolved in 10 ml of methanol. Subsequently, ice-cold water was added to the methanol solution in 1-ml increments until a precipitate was formed. The slurry was filtered and dried. The purity of the product was analyzed by thin layer chromatography (TLC) on silica gel plates (Silica Gel-70 F254, Wako Pure Chemical Industries, Osaka, Japan) using 1-butanol/acetic acid/H_2O (5:2:3 in volume) as the developing solvent, and the R_f value was 0.82. FAB-Mass and infrared spectroscopy analyses confirmed that 4,4′-azobenzene-dimaleimide (ABDM) was synthesized.

SDS-PAGE—Electrophoresis was performed in 7.5–20% polyacrylamide gradient slab gels in the presence of 0.1% sodium dodecylsulphate (SDS) at a constant voltage (200 V) in the discontinuous buffer system of Laemmli (*34*).

Photoirradiation for Cis-Trans Isomerization of ABDM—Isomerization of ABDM was performed at 0°C by UV light irradiation using a Blak-ray lamp (16 W) (UVP Inc., San Gabriel, USA) at 366 nm for formation of the cis isomer and by VIS light irradiation using a room fluorescent lamp (27 W) for formation of the trans isomer.

ATPase Assay of S1—The ATPase activity of myosin heads (S1) was measured at 25°C in a reaction mixture comprising 0.5 M KCl, 30 mM Tris-HCl (pH 7.5), 1 μM S1 (or ABDM-S1), 5 mM $MgCl_2$ ($CaCl_2$ or EDTA), and 2 mM ATP. The reaction was stopped by the addition of 10% trichloroacetic acid, and the released phosphate (P_i) was measured by the method of Youngburg and Youngburg (*35*).

Crosslinking of SH1 and SH2 in S1 with ABDM—Crosslinking of the SH1 and SH2 residues in S1 with ABDM was carried out by reacting 30 μM S1 and 90 μM ABDM in the presence of 10 mM imidazole-HCl (pH 7.0), 10 mM KCl, 1mM $MgCl_2$, 2% DMF and 1 mM ADP for 40 min at 0°C. The reaction was stopped by adding dithiothreitol (DTT) to a final concentration of 2 mM. The crosslinked S1 (ABDM-S1) was isolated from unreacted reagents with a Sephadex G-50 column or a Sephacryl S-300 column equilibrated with 30 mM Tris-HCl (pH 7.5) and 120 mM NaCl. The stoichiometry of the incorporated ABDM as to S1 was determined from the absorption spectrum using an extinction coefficient of 22,900 M^{-1} cm^{-1} at 342 nm.

X-Ray Solution Scattering of S1 Samples—X-ray solution scattering experiments on papain-digested S1 were performed at 19°C with a small-angle diffractometer installed in the beam line 15A1, using synchrotron radiation at the Photon Factory, KEK (Tsukuba, Japan), according to the method of Wakabayashi *et al.* (*1*). The X-ray scattering intensities of S1 samples were measured with camera lengths of 2.33 m for the small angle region and 1.5 m for the medium angle region with a one-dimensional position sensitive detector (Rigaku, Tokyo). The intensity curves obtained with the long and short camera lengths were connected to obtain a scattering curve in the wide range up to the scattering vector length $S = 0.04$ $Å^{-1}$ [$S = 2\sin\theta/\lambda$, where 2θ is the scattering angle and λ is the wavelength of monochromatized X-rays (1.50 Å) used]. The protein concentration of the S1 sample was varied from 3 to 12 mg/ml. Each sample was centrifuged just before X-ray experiments to remove any aggregates.

As control experiments, samples of intact S1 without any nucleotide and in the presence of MgATP were examined. The apparent radius of gyration (R_g) of S1 was calculated from the slope of the linear region in the Guinier plot ($\ln[I(S)]$ *vs.* S^2) of scattering intensity data [$I(S)$] at any protein concentration (c) (*36*). The true R_g value was determined by extrapolating the apparent R_g value to zero protein concentration (c = 0). The $I(0)/c$ value obtained on extrapolation of the Guinier straight line to S = 0 was used as a measure of the molecular weight of S1. A Kratky plot [$S^2I(S)$ *vs.* S] of scattering intensity data (*36*) was made to observe any shape changes of S1 crosslinked with ABDM. The pair distance distribution function [$p(r)$] was calculated by indirect Fourier transformation of $I(S)$ (*37*). The maximum chord length (D_{max}) of S1 was estimated from the r-intercept of the $p(r)$ function.

RESULTS

Spectoscopic Properties of Free 4,4'-Azobenzene-Dimaleimide (ABDM)—We have synthesized a thiol specific, bifunctional photochromic crosslinker, 4,4′-azobenzenedimaleimide (ABDM). *Cis-trans* photoisomerization of ABDM should have an effect to alter the crosslinking distance from 5 to 17 Å, as depicted in Fig. 1.

It is well known that the configuration of the azobenzene molecule changes on photoirradiation; trans to *cis* formation is induced by UV light irradiation and *cis* to *trans* formation by VIS light irradiation (*25*, *26*). The configurational state (*cis* or *trans*) of azobenzene and its derivatives can be monitored by UV/VIS light absorption spectroscopy (*26*, *38*). The UV/VIS absorbance spectra for ABDM were similar to those characteristic of azobenzene. Figure 2A shows an absorption spectrum of the trans form of ABDM in a 70% ethanol solution (solid line). The absorption maximum of the *trans*-ABDM was

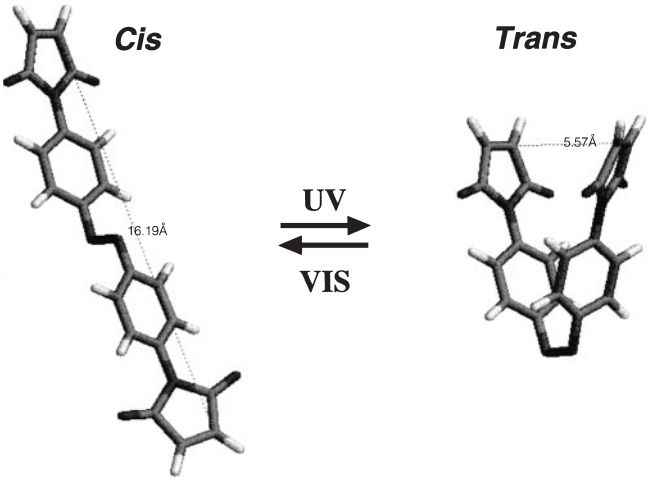

Fig. 1. **Chemical structure of 4,4′-azobenzene-dimaleimide (ABDM).** The chord length of the molecule is ~5 Å for the *cis* form and ~17 Å for the *trans* form.

345 nm whereas azobenzene exhibited a maximum at 315 nm under the same conditions. UV light (366 nm) irradiation of the *trans*-ABDM solution with the Blak-ray lamp (16 W) led to a marked reduction in the peak at 345 nm over time. After irradiation for 5 min, alteration of the spectrum was saturated. On comparison with published spectra data (*39*), it was estimated that the solution after 5 min irradiation contained approximately 75% *cis* form and 25% *trans* form of ABDM.

In the dark, the *cis* form of ABDM was relatively stable, and even after 30 min at 24°C, the recovery of the spectrum to that of the trans form was just 10–15% (Fig. 2B). On the contrary, 5 min VIS light irradiation of the ABDM solution containing predominantly the cis form led to an almost complete isomerization to the trans form (Fig. 2C).

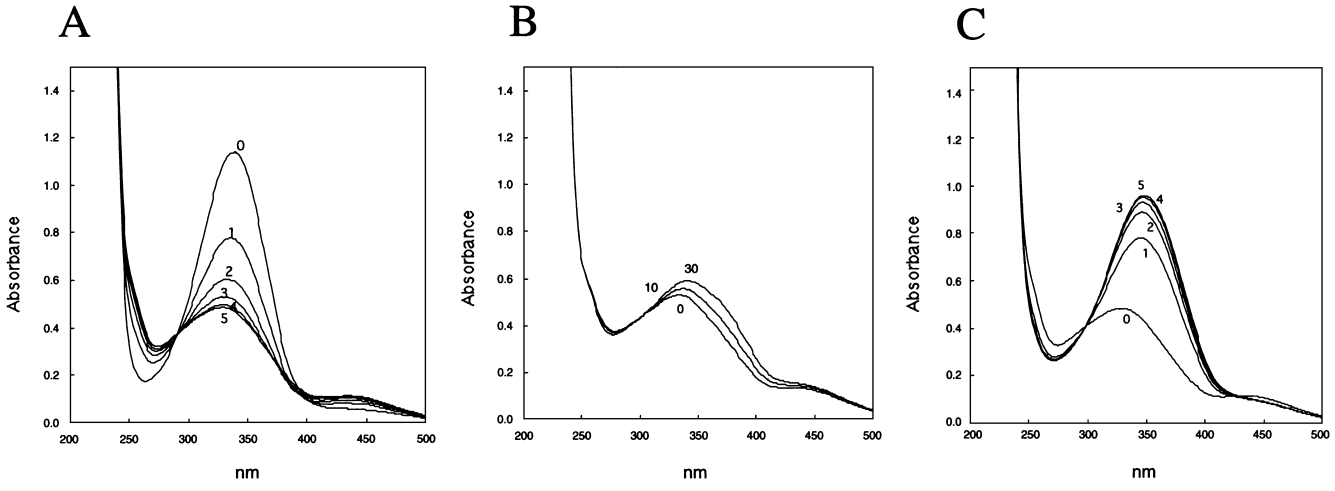

Fig. 2. **A: Changes in the absorption spectrum of free ABDM induced by UV light irradiation.** The free ABDM (50 μM) in 70% ethanol was irradiated with a UV lamp (Blak-ray lamp, 16 W) at 366 nm for 0, 1, 2, 3, 4 and 5 min at room temperature. B: Recovery of the absorption spectrum of free ABDM irradiated with UV light in the dark. The free ABDM (50 μM) in 70% ethanol was irradiated with UV light at 366 nm for 5 min. Subsequently, the time course of recovery of the absorption spectrum resulting from the cis to trans isomerization was measured in the dark for 0, 10 and 30 min at room temperature. C: Cis to trans isomerization of free ABDM induced by VIS light irradiation. Free *cis*-ABDM (50 μM) in 70% ethanol was prepared by UV light irradiation for 5 min at room temperature. Formation of the *cis*-ABDM with a fluorescent room lamp for 0, 1, 2, 3, 4 and 5 min at room temperarure was observed.

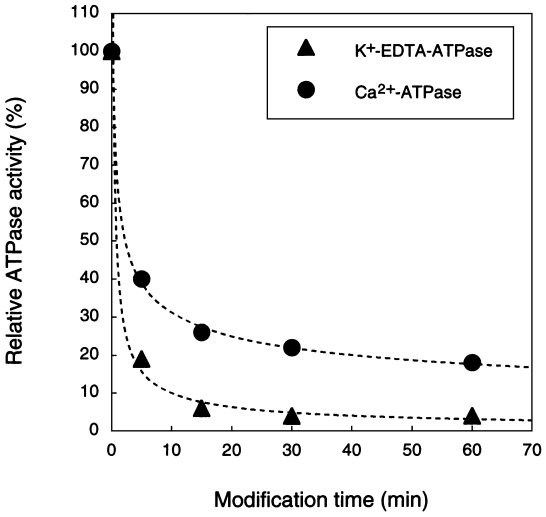

Fig. 3. **Effect of crosslinking with ABDM on the EDTA(K^+)-EDTA-ATPase and Ca^{2+}-ATPase activities of S1.** The relative activities were measured at 25°C in a solution comprising 1 μM S1, 2 mM ATP, 0.5 M KCl, and 50 mM Tris-HCl (pH 7.5) in the presence of 5 mM EDTA and $CaCl_2$, respectively.

Crosslinking of SH1 and SH2 in S1 with ABDM—It is known that SH1 and SH2 of S1 can be crosslinked with several bifunctional reagents (*17*, *19*), and the crosslinking conditions have well been studied for the compound *p*PDM (*18*, *40*). ABDM has a structure possessing two SH specific maleimide groups similar to but with a slightly longer crosslinking span than in the case of *p*PDM. Following the method for crosslinking with *p*PDM as described under "MATERIALS AND METHODS," crosslinking between SH1 and SH2 with ABDM was performed. Prior to the reaction, the ABDM was irradiated with UV light in order to prepare the cis-form of ABDM. S1 was reacted with UV-irradiated ABDM in the dark, the crosslinking reaction being monitored by measuring alterations in the Ca^{2+}- and EDTA (K^+)-ATPase activities. The effect of modification of the reactive cysteine residues (SH1 and SH2) on the ATPase activity of skeletal muscle myosin S1 has been well investigated (*41*): (i) modification of only SH1 with several kinds of cysteine-specific reagents leads to elevation of the Ca^{2+}-ATPase activity and simultaneously reduces the EDTA (K^+)-ATPase activity, (ii) modification of only SH2 reduces the EDTA (K^+)-ATPase activity but does not affect the Ca^{2+}-ATPase activity, and (iii) when both residues are modified, the Ca^{2+}-ATPase and EDTA (K^+)-ATPase activities are both reduced. Fig. 3 shows the results of crosslinking of S1 with ABDM (ABDM-S1) showing typical alterations of both ATPase activities, which indicate the simultaneous modification of both cysteine residues. The stoichiometry of the incorporated ABDM as to S1 was estimated from the absorption spectra using the extinction coefficient of ABDM as described under "MATERIALS AND METHODS." For the modification time of 60 min, the molar ratio of incorporated ABDM : S1 was approximately 1:1.1, confirming that both SH1 and SH2 in S1 were modified with ABDM.

UV/VIS Light Absorption Spectra of S1 Crosslinked with ABDM—UV/VIS light spectra of S1 crosslinked with ABDM were measured and compared with those of free ABDM. UV light irradiation of the ABDM-S1complex gave rise to a spectrum similar to that seen with free ABDM (Fig. 4A). Although the absorption of the ABDM-S1 complex at 280 nm was much greater than that of free ABDM, the absorption maximum at 342 nm was not altered by the presence of S1 and thus the changes around the ABDM moiety could be quantitatively monitored. The velocity of isomerization for the incorporated ABDM from the *trans* to the *cis* form was

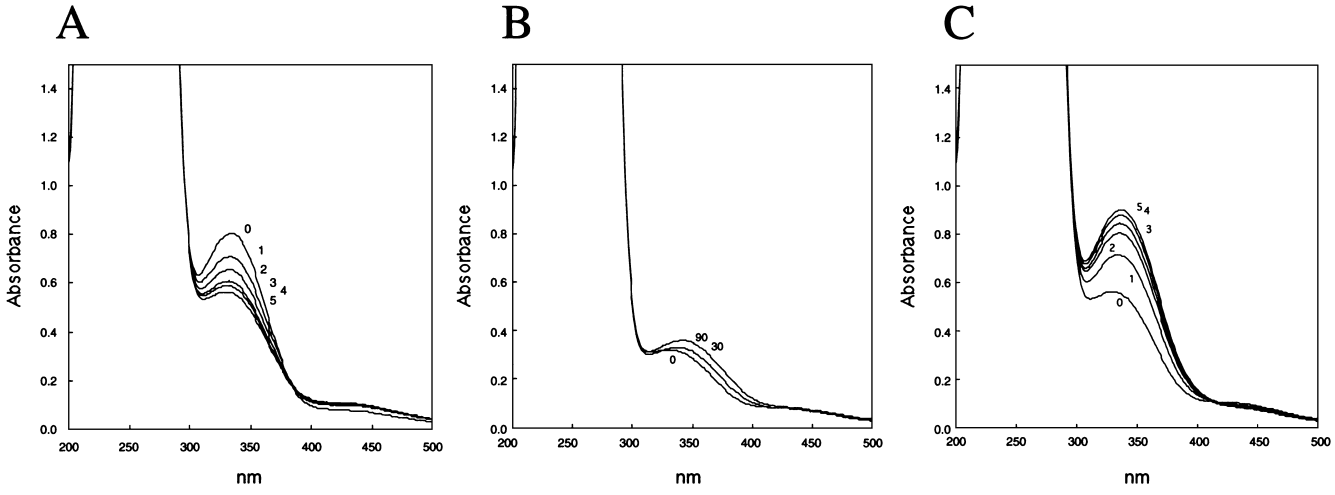

Fig. 4. **A: Changes in the absorption spectrum of the ABDM-S1 complex induced by UV light irradiation.** The ABDM-S1 (50 μM) complex was irradiated with a UV lamp (Blak-ray lamp 16 W) at 366 nm for 0, 1, 2, 3, 4 and 5 min at room temperature in a solution of 120 mM NaCl and 30 mM Tris-HCl (pH 7.5). B: Recovery of the absorption spectrum of ABDM-S1 irradiated with UV light in the dark. The ABDM-S1 (50 μM) in a solution comprising 120 mM NaCl and 30 mM Tris-HCl (pH 7.5) was irradiated with UV light at 366 nm for 5 min. Subsequently, the time course following the *cis* to *trans* isomerization was measured in the dark for 0, 30 and 90 min at room temperature. C: Changes in the absorption spectrum resulting from the cis to trans isomerization of free ABDM induced by VIS light irradiation. The cis-ABDM-S1 (50 μM) in a solution of 120 mM NaCl and 30 mM Tris-HCl (pH 7.5) was prepared by UV light irradiation for 5 min at room temperature. Formation of *cis*-ABDM-S1 with a fluorescent room lamp for 0, 1, 2, 3, 4 and 5 min at room temperature was observed.

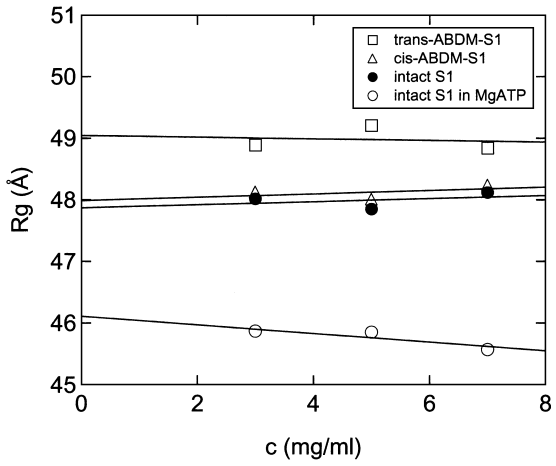

Fig. 5. **Protein concentration dependence of the radii of gyration (R_g) of various S1 samples.** The apparent radii of gyration values calculated from the slopes of the straight lines in the Guinier plots of X-ray scattering intensity data were plotted against the protein concentration (c). Open squares, *trans*-ABDM-S1; open triangles, cis-ABDM-S1; solid circles, intact S1 without any nucleotide; open circles, intact S1 in the presence of ATP. Each straight line was obtained by least squares fitting to the data points. The true R_g values of these S1 samples were obtained by extrapolating the straight lines to $c = 0$.

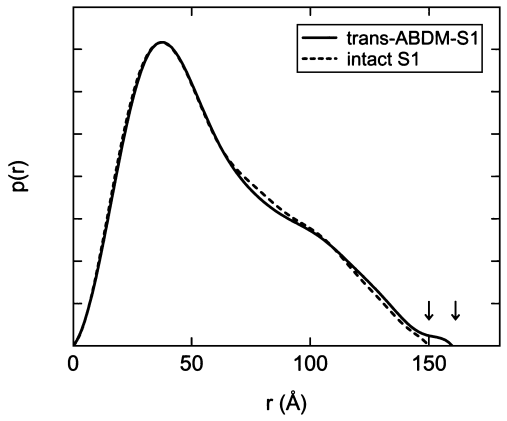

Fig. 6. **Pair-distance distribution functions [$p(r)$] of *trans*-ABDM-S1 and intact S1.** The $p(r)$ function of the *trans*-ABDM-S1 sample is shown superimposed on that of the intact S1 without any nucleotide. Solid line curve, $p(r)$ function of *trans*-ABDM-S1; dotted line curve, that of intact S1. Arrows indicate the maximum chord lengths (D_{max}) of the S1 samples.

almost identical to that of free ABDM. On the contrary, the isomerization velocity for the incorporated ABDM from the *cis* to the *trans* form was about twofold slower than that for free ABDM (Fig. 4C). In the dark, the recovery of the absorption spectrum of the incorporated ABDM was also slower (approximately three times) than that of free ABDM (Fig. 4B).

Localized Conformational Changes of S1 Induced by Photoisomerization of ABDM Crosslinking SH1 and SH2—We have studied the conformational changes on the myosin head induced by the *cis-trans* isomerization of ABDM crosslinking SH1 and SH2. The Mant-ADP trapped within the ATP binding sites was not released on *cis-trans* isomerization of the crosslinked ABDM (data not shown), suggesting no great change at the ATP binding sites in both samples. In experiments on the cosedimentation of actin and the ABDM-S1 complex, no difference in the affinity to actin was detected between the *cis*-ABDM-S1 and *trans*-ABDM-S1, suggesting there were no great conformational differences in the actin binding sites in both S1 samples (data not shown). We have also tried to detect other conformational changes in the motor domain using fluorescent probes [prodan and FHS labeled at lysine (Lys) 553], but did not observe any appreciable change. We have measured circular dichroism (CD) spectra for the *cis*-ABDM-S1 and *trans*-ABDM-S1 to find any differences in their helical contents. Unfortunately, the changes expected in a short helical segment of the SH1 helix were hard to show due to the largeα-helix content of S1.

Small-Angle X-Ray Solution Scattering of the ABDM-S1 Complexes—The global conformational change of the ABDM-S1 complex induced on *cis-trans* isomerization of the crosslinked ABDM was investigated by means of a small-angle X-ray scattering technique using synchrotron radiation as the intense X-ray source. Previously, from the radius gyration (R_g) and the pair-distance distribution function determined from X-ray scattering intensity data, Wakabayashi and colleagues (*1*, *2*) clearly showed that the molecular shape of the myosin head (S1) changed to a more compact or rounded form in the presence of ATP, and that the bending occurred between the motor domain and the regulatory domain. They also showed that similar compaction of the molecule occurred upon formation of ternary complexes of S1 with ADP and AlF_4^- (S1·ADP·AlF_4^-), S1 with ADP and BeFn (S1·ADP·BeFn), and S1 with ADP and vanadate (S1·ADP·Vi), which mimic key intermediates in the myosin ATPase cycle (*1*, *2*). The global changes of these complexes were consistent with the X-ray crystal structure analyses of them except in the case of the S1·ADP·BeFn complex (*8*, *9*, *13*, *14*). We analyzed the solution structures of the *cis*-ABDM-S1 and *trans*-ABDM-S1 complexes by small-angle X-ray scattering. Prior to the X-ray scattering experiments, papain-digested S1 was crosslinked with *cis*-ABDM that had been irradiated with UV light and the excess ABDM was removed by gel filtration. The samples were kept in the dark on ice. Then the ABDM-S1 sample was irradiated with VIS or UV light to induce *trans*-ABDM-S1 or cis-ABDM-S1, respectively, and X-ray experiments were performed on this sample. X-ray measurements on the *cis*-ABDM-S1 complex were performed in the dark. The Guinier plots of the scattering intensity data for the *cis*-ABDM-S1 complex, the *trans*-ABDM-S1complex together with intact S1 (without any nucleotide), and S1 in the presence of ATP all produced straight lines in the range of $S^2 \leq 0.20 \times 10^{-4}$ Å^{-2}, and the extrapolated $I(0)/c$ values were almost the same, indicating the lack of aggregation in any S1 solution (data not shown). The apparent radius of gyration (R_g) was calculated from the linear slope of the Guinier plots in the range of $0.004 \times 10^{-4} \leq S^2 \leq 0.203 \times 10^{-4}$ Å^{-2}, and it was plotted against the protein concentration (c) (Fig. 5). When extrapolated to $c = 0$, the true R_g value of the *cis*-ABDM-S1 complex was about 48.0 Å, *i.e.* very close to that of the intact S1 (~47.8 Å), which is well

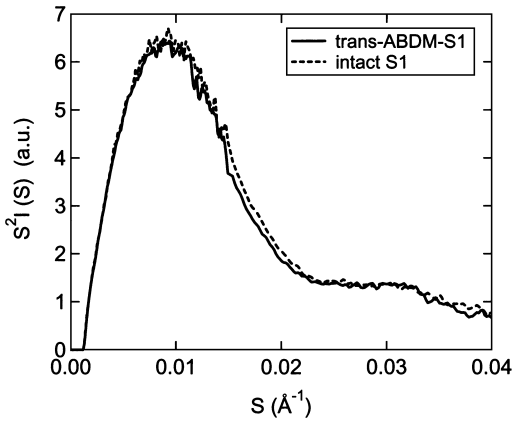

Fig. 7. **Kratky plots of the X-ray scattering intensity data of the *trans*-ABDM-S1 and intact S1 samples.** Solid line curve, *trans*-ABDM-S1; Dotted line curve, the intact S1.

comparable with the previously reported values (*1*, *42*). On the contrary, the true R_g value of the *trans*-ABDM-S1 complex was about 49.0 Å, *i.e.* distinctly larger, by ~1 Å, than the *cis*-ABDM-S1 and the intact S1. The intact S1 in the presence of ATP showed a large decrease (~2 Å) in R_g, comparable to the previously reported change (*1*, *42*). As mentioned above, assuming that the *cis*-ABDM-S1 sample contains about 25% of *trans*-ABDM-S1 and the *trans*-ABDM-S1 sample contained little of the *cis*-form, correction yields a R_g value of 47.7 Å for the *cis*-ABDM-S1 complex (see "DISCUSSION"). Thus the *cis*-ABDM-S1 exhibited a very small change in R_g. Figure 6 compares the pair-distance distribution functions [$p(r)$] of the *trans*-ABDM-S1 complex and the intact S1. The $p(r)$ curve of the *trans*-ABDM-S1 complex intersected the intact S1 curve at r ~110 Å. Beyond this, there were siginificantly more vector lengths than for the intact S1, resulting in the maximum chord length (D_{max}) (indicated by arrows in Fig. 6), *i.e.* longer by about 10 Å. Figure 7 shows Kratky plots of the scattering intensity data for the *trans*-ABDM-S1 and intact S1 samples. Consistent with elongation of the molecule, there was a difference between the two Kratky plots in the range of $0.006 < S < 0.025$ Å^{-1}, revealing a shape change of the *trans*-ABDM-S1 complex. Comparison of the Kratky plots of the *trans*-ABDM-S1 and the intact S1 in the presence of ATP indicates that the bending of the lever arm portion in the *trans*-ABDM-S1 occurs in the opposite direction to its swing in S1 induced on the binding of ATP (data not shown). Thus the data clearly demonstrated that the cis-trans isomerization of ABDM incorporated into the SH1-SH2 region of S1 caused movement of the regulatory domain relative to the catalytic domain.

DISCUSSION

This is the first report on the use of a photochromic group to induce intrinsic conformational changes in the ATP-driven molecular motor of myosin in the absence of ATP. Recent X-ray crystallographic (*10–14*) and point mutation studies on myosin motor domains (*15*, *16*) have provided important information on the mechanical transduction from ATP chemical energy to the swing of the lever arm. Therefore we expect that the introduction of the mechanical energy input unit into the energy transducing region, which acts like a cam-shaft, may drive the motor protein without ATP. Supporting this idea, it has been reported that the incorporation of photochromic groups into other enzymes photomodulates their activity, e.g. papain and glucose oxidase (*2*, *43*). A problem with using photochromic crosslinkers is whether or not they can be specifically introduced in sites. Fortunately, the myosin motor domain has reactive cysteines (SH1 and SH2) that are thought to be located on one of the energy transducing sites (*21*). Moreover, it is well known that SH1 and SH2 can be crosslinked with several kinds of bifunctional reagents (*17–19*). We have designed a bifunctional photochromic crosslinker containing an azobenzene moiety with two thiol-specific maleimides at the 4 and 4′ positions of azobenzene to permit crosslinkage of SH1 and SH2. We chose azobenzene as the photochromic group because it undergoes reversible isomerization between the *cis* and *trans* forms, leading to an extreme alteration in the molecular size. The distance between the two *para*-carbon atoms of the azobenzene unit in the *trans* configuration is 9 Å and it is 5 Å in the *cis* configuration (see Fig. 1). Previously, Kumita *et al.* (*27*) and Flint et al. (*28*) demonstrated that a similar bifunctional photochromic compound, 4,4′-diiodoacetamide-azobenzene, crosslinked two cysteine residues in a peptide, and photoisomerization of the compound from the *trans* to the *cis* form caused a large increase in the helical content of the peptide (*27–28*). From the structural similarity between ABDM and the crosslinker reported by Kumita *et al.* (*27*), we expect that the *cis-trans* isomerization of ABDM can induce a conformational change in the SH1-SH2 region of a myosin motor domain leading to a global change in the molecular shape.

ABDM was incorporated into S1 at the molar ratio of approximately 1:1. The crosslinking between SH1 and SH2 was confirmed by the inhibition of the Ca^{2+}-ATPase and EDTA (K^+)-ATPase activities of S1. The crosslinking of S1 with ABDM caused a reduction in the time course of the ATPase activities of S1 similarly to in the case of crosslinking with *p*PDM (*44*, *45*) (Fig. 3). Further evidence for modification to both cysteines in S1 with ABDM was that the fluorescent probes BD (6-bromoacetyl-2-dimethyl-aminonaphthalene) and AD (6-acryloyl-2-dimethylaminonaphthalene), which are specific for SH1 and SH2, respectively (*46*), were not incorporated into S1 modified with ABDM (data not shown).

We have examined the localized conformational changes on the myosin head induced by *cis-trans* isomerization of ABDM crosslinking SH1 and SH2. At low ionic strength, there was no difference in affinity to actin between *cis*-ABDM-S1 and *trans*-ABDM-S1, indicating that little conformational change occurred around the actin binding sites of S1. Since the Mant-ADP trapped within the ATP binding sites of S1 was not released on *cis-trans* isomerization of the crosslinked ABDM (data not shown), the conformational change around the SH1-SH2 moiety caused by the *cis-trans* isomerization does not significantly affect the conformation of the ATPase sites. We have also tried to detect other conformational changes in the motor domain using fluorescent probes

(prodan and FHS (6-[fluorescein-5(and *6*)-carboxyamido]hexanoic acid succinimidylester) labeled at Lys 553), but observed little change. On the other hand, X-ray solution scattering revealed a small but distinct global conformational change of the myosin head during the *cis-trans* isomerization (Figs. 5–7). The Kratky plots of X-ray scattering data (Fig. 7) revealed a shape change of the *trans*-ABDM-S1 complex, suggesting that the localized conformational change of S1 produced on the *cis* to *trans* isomerization causes a slight but significant swing of the lever arm portion in the opposite direction to that seen in the presence of ATP. The *cis*-ABDM-S1 sample showed a comparable R_g value to that of the intact S1 (see Fig. 5). The *cis*-ABDM-S1 sample produced on irradiation with UV light contained about 25% *trans* form. From the weighted additivity law of $R_{g\,obs}^2 = \alpha R_{g\,cis}^2 + \beta R_{g\,trans}^2$ (α and β, and $R_{g\,cis}$ and $R_{g\,trans}$ denote the fractions and the true R_g values of *cis* and trans species, respectively), the R_g value ($R_{g\,cis}$) of the *cis*-ABDM-S1 complex is estimated to 47.7 Å, this being smaller by about 0.3 Å than that of the *cis*-rich ABDM-S1. Thus the *cis*-ABDM-S1 may exhibit a very small change toward to the compact form.

According to the results of recent X-ray crystallographic studies on various forms of S1 (*12–14*), small conformational changes in the switch II loop can cause a rotational motion of the 50 kDa lower domain and the relay helix, and one end of the 50 kDa domain can deliver torque from the switch II loop to the converter domain. From these crystallographic implications, it has been suggested that the relay helix, the converter domain and the SH1-helix make up a transmission module.

It has been suggested that the region that encompasses the reactive SH1 and SH2 residues can structurally fluctuate in the presence of bound nucleotides (*9*). Indeed, both forms of ABDM crosslinked the SH1 and SH2 of S1. A significant alteration of the lever arm of S1 was produced by the trans form of ABDM. As the SH1 and SH2 groups sit on the two different helices in the motor domain and each thiol group protrudes from the opposite side of the SH1-helix, the crosslinking of SH1 and SH2 by *trans*-ABDM may generate a kink between the two thiol groups so that the SH1 and SH2 groups are oriented on the same side. Subsequently, if the kink directly causes rotation of the converter domain through a distortion in the SH1-SH2 region, it is possible that the lever arm portion swings in the opposite direction from that induced by ATP binding. Supporting this idea, Sugimoto *et al.* (*47*, *48*) showed on X-ray small-angle scattering that skeletal myosin S1 crosslinked with *p*PDM, which has a shorter crosslinking span (12 Å) than ABDM, had slightly larger R_g and D_{max} values than those of unmodified S1. And as a control, the S1 of which SH1 and SH2 were modified by monofunctional thiol reagent *N*-ethylmaleimide (NEM) showed a slightly smaller R_g than that of intact S1 and an almost identical value to S1-MgADP (Sugimoto *et al*., manuscript in preparation). They suggested a swing of the lever arm of S1 in the opposite direction from that induced by ATP, consistent with the observation for the crystal structure of scallop S1 crosslinked with *p*PDM in the presence of a nucleotide (*12*, *14*).

The crystal structure of scallop myosin S1 crosslinked with *p*PDM showed that the SH1 helix assumed an unwound conformation. Although the CD spectra for the *cis*- and *trans*-ABDM-S1 failed to reveal a change in the helical content of the SH1 helix due to the large α-helix content of S1, the unwound conformation of the SH1 helix would be induced on isomerization of crosslinked ABDM, resulting in a swing of the lever arm in the opposite direction to that observed in the presence of ATP. The lack of conformational changes in the motor domain of ABDM-S1 implies that the conformational change around the SH1 and SH2 region produced by the isomerization may not be transmitted to the motor domain. Himmel *et al.* (*13*) stated that S1 may be assumed to have an "internal-uncoupled conformation," which effectively disengages the converter/lever arm module from the motor when the SH1 helix unwinds. The ABDM-S1 may be in a state similar to the "internal-uncoupled conformation."

We synthesized a cysteine-specific bifunctional photochromic crosslinker, 4,4′-azobenzene-dimaleimide, and incorporated it into the energy transmission module of the ATP-driven motor domain of skeletal muscle myosin. A small but significant swing of the lever arm of myosin head was induced on *cis-trans* isomerization of the photochromic group. It was shown that the incorporated photochromic group partially acts as a mechanical energy input in a motor protein. The photochromic molecule may be applicable to other energy transducing and regulatory portions of proteins.

This work was supported by Grants-in-Aid for Scientific Research C (14580677) from the Ministry of Education, Science, Sports and Culture of Japan (SM). The SAXS experiment was approved by Photon Factory Advisory Committee (No. 2001G369) and supported in part by the Special Coordination Funds from the Ministry of Education, Science, Sports and Culture of Japan (KW). We thank Dr. Janet R. Kumita and Dr. G. Andrew Woolley (Department of Chemistry, University of Toronto) for helpful discussion on the work.

REFERENCES

1. Wakabayashi, K., Tokunaga, M., Kohno, I., Sugimoto, Y., Hamanaka, T., Takezawa, Y., Wakabayashi, T., and Amemiya, Y. (1992) Small-angle synchrotron x-ray scattering reveals distinct shape changes of the myosin head during hydrolysis of ATP. *Science* **258**, 443–447
2. Sugimoto, Y., Tokunaga, M., Takezawa, Y., Ikebe, M., and Wakabayashi, K. (1995) Conformational changes of the myosin heads during hydrolysis of ATP as analyzed by x-ray solution scattering. *Biophys. J.* **68**, 29s–34s
3. Katayama, E. (1998) Quick-freeze deep-etch electron microscopy of the actin-heavy meromyosin complex during the in vitro motility assay. *J. Mol. Biol.* **278**, 349–367
4. Xing, J. and Cheung, H.C. (1995) Internal movement in myosin subfragment 1 detected by fluorescence resonance energy transfer. *Biochemistry* **34**, 6475–6487
5. Perkins, W.J., Weiel, J., Grammer, J., and Yount, R.G. (1984) Introduction of a donor acceptor pair by a single protein modification. Forster energy transfer distance measurements from trapped 1, N6-ethenoadenosine diphosphate to chromophoric cross-linking reagents on the critical thiols of myosin subfragment. *J. Biol. Chem.* **259**, 8786–8793
6. Suzuki, Y., Yasunaga, T., Ohkura, R., WakAabayashi, T., and Sutoh, K. (1998) Swing of the lever arm of a myosin motor at the isomerization and phosphate-release steps. *Nature* **396**, 380–383
7. Xiao, M., Li, H., Snyder, G.E., Cooke, R., Yount, R.G., and Selvin, P.R. (1998) Conformational changes between the

active-site and regulatory light chain of myosin as determined by luminescence resonance energy transfer: the effect of nucleotides and actin. *Proc. Natl Acad. Sci. USA* **95**, 15309–15314
8. Fisher, A.J., Smith, C.A., Thoden, J.B., Smith, R., Sutoh, K., Holden, H.M., and Rayment, I. (1995) X-ray structures of the myosin motor domain of Dictyostelium discoideum complexed with MgADP-BeF_x and MgADP-AlF_4^-. *Biochemistry* **34**, 8960–8972
9. Smith, C.A. and Rayment, I. (1996) X-ray structure of the magnesium (II).ADP.vanadate complex of the Dictyostelium discoideum myosin motor domain to 1.9 Å resolution. *Biochemistry* **35**, 5404–5417
10. Rayment, I., Rypniewski, W.R., Schmidt-Base, K., Smith, R., Tomchick, D.R., Benning, M.M., Winkelmann, D.A., Wasenberg, G., and Holden, H.M. (1993) Three-dimensional structure of myosin subfragment-1: a molecular motor. *Science* **261**, 50–58
11. Dominguez, R., Freyzon, Y., Trybus, K.M., and Cohen, C. (1998) Crystal structure of a vertebrate smooth muscle myosin motor domain and its complex with the essential light chain: visualization of the pre-power stroke state. *Cell* **94**, 559–571
12. Houdusse, A., Kalabokis, V.N., Himmel, D., Szent-Gyorgyi, A.G., and Cohen, C. (1999) Atomic structure of scallop myosin subfragment S1 complexed with MgADP: a novel conformation of the myosin head. *Cell* **97**, 459–470
13. Himmel, D.M., Gourinath, S., Reshetnikova, L., Shen, Y., Szent-Gyorgyi, A.G., and Cohen, C. (2002) Crystallographic findings on the internally uncoupled and near-rigor states of myosin: further insights into the mechanics of the motor. *Proc. Natl Acad. Sci. USA* **99**, 12645–12650
14. Houdusse, A., Szent-Gyorgyi, A.G., and Cohen, C. (2000) Three conformational states of scallop myosin S1. *Proc. Natl Acad. Sci. USA* **97**, 11238–11243
15. Sasaki, N., Ohkura, R., and Sutoh, K. (2003) Dictyostelium myosin II mutations that uncouple the converter swing and ATP hydrolysis cycle. *Biochemistry* **42**, 90–95
16. Ito, K., Uyeda, T.Q., Suzuki, Y., Sutoh, K., and Yamamoto, K. (2003) Requirement of domain-domain interaction for conformational change and functional ATP hydrolysis in myosin. *J. Biol. Chem.* **278**, 31049–31057
17. Cheung, H.C., Gryczynski, I., Malac, H., Wiczk, W., Johnson, M.L., and Lakowicz, J.R. (1991) Conformational flexibility of the Cys 697-Cys 707 segment of myosin subfragment-1. Distance distributions by frequency-domain fluorometry. *Biophys. Chem.* **40**, 1–17
18. Reisler, E., Burke, M., Himmelfarb, S., and Harrington, W.F. (1974) Spatial proximity of the two essential sulfhydryl groups of myosin. *Biochemistry* **13**, 3837–3840
19. Wells, J.A. and Yount, R.G. (1982) Chemical modification of myosin by active site trapping of metal-nucleotides with thiol crosslinking reagents. *Methods Enzymol.* **85**, 93–116
20. Uyeda, T.Q.P., Abramson, P.D., and Spudich, J.A. (1996) The neck region of the myosin motor domain acts as a lever arm to generate movement. *Proc. Natl Acad. Sci. USA* **93**, 4459–4464
21. Hiratsuka, T. (1993) Behavior of Cys-707 (SH1) in myosin associated with ATP hydrolysis revealed with a fluorescent probe linked directly to the sulfur atom. *J. Biol. Chem.* **268**, 24742–24750
22. Ichimura, K., Seki, T., Kawanishi, Y., Suzuki, Y., Sakuragi, M., and Tamaki, T. (1996) Photocontrol of liquid crystal alignment by "command surface" in *Photoreactive Materials for Ultrahigh Density Optical Memory* (Irie, M., ed.) pp. 55–83, Elsevier, Amsterdam
23. Irie, M., Fukaminato, T., Sasaki, T., Tamai, N., and Kawai, T. (2002) A digital fluorescent molecular photoswitch. *Nature* **420**, 759–760
24. Kimura, K., Mizutani, R., Suzuki, T., and Yokoyama, M. (1998) Photochemical ionic-conductivity switching systems of photochromic crown ethers for informatiAon technology. *J. Inclusion Phenomena Mol. Recognition Chem.* **32**, 295–310
25. Rau, H. (1990) Photochromism in *Molecules and Systems* (Durr, H. and Bouas-Laurent, H., Aeds.) pp. 165–192, Elsevier, Amsterdam
26. Rau, H. (1990) in *Photochemistry and Photophysics* (Rabeck, J.F., ed.) Vol. II, pp. 119–141, CRC, Boca Raton, FL
27. Kumita, J.R., Smart, O.S., and Woolley, G.A. (2000) Photo-control of helix content in a short peptide. *Proc. Natl Acad. Sci. USA* **97**, 3803–3808
28. Flint, D.G., Kumita, J.R., Smart, O.S., and Woolley, G.A. (2002) Using an azobenzene cross-linker to either increase or decrease peptide helix content upon trans-to-cis photoisomerization. *Chem. Biol.* **9**, 391–397
29. Perry, S.V. (1952) Myosin adenosine triphosphatase. *Methods Enzymol.* **2**, 582–588
30. Weeds, A.G. and Taylor, R.S. (1975) Separation of subfragment-1 isoenzymes from rabbit skeletal muscle myosin. *Nature* **257**, 54–56
31. Margossian, S.S. and Lowey, S. (1982) Preparation of myosin and its subfragments from rabbit skeletal muscle. *Methods Enzymol.* **85**, 55–71
32. Pardee, J.D. and Spudich, J.A. (1982) Purification of muscle actin. *Methods Enzymol.* **85**, 164–168
33. Nishimura, J.S., Petrich, J.A., Milne, A.F., and Mitchell, T. (1978) N, N′-*o*-phenylenedi[1,4-^{14}C]maleimide. Its synthesis and application in the cross-linking of *Escherichia coli* succinic thiokinase. *Int. J. Biochem.* **9**, 93–96
34. Laemmli, U.K. (1970) Cleavage of structural proteins during the assembly of the head of bacteriophage T4. *Nature* **227**, 680–685
35. Youngburg, G.E. and Youngburg, M.V. (1930) A system of blood phosphorus analysis. *J. Lab. Clin. Med.* **16**, 158–166
36. Feigun, L.A. and Svergun, D.I. (1987) *Structure Analysis by Small-Angle X-Ray and Neutron Scattering*, Plenum Press, New York
37. Svergun, D.I. (1992) Determination of the regularization parameter in indirect-transform methods using perceptual criteria. *J. Appl. Crystallogr.* **25**, 495–503
38. Zimmerman, G., Chow, L.Y., and Paik, U.J. (1958) The photochemical isomerization of azobenzene. *J. Amer. Chem. Soc.* **80**, 3528–3531
39. Behrendt, R., Renner, C., Schenk, M., Wang, F., Wachtveitl, J., Oesterhelt, D., and Moroder, L. (1999) Photomodulation of the conformation of cyclic peptides with azobenzene moieties in the peptide backbone. *Angew. Chem. Int. Ed. Engl.* **38**, 2771–2774
40. Burke, M. and Sivaramakrishnan, S. (1981) Subunit interaction in myosin subfragment 1. *J. Biol. Chem.* **256**, 8859–8862
41. Reisler, E., Burke, M., and Harrington, W.F. (1974) Cooperative role of two sulfhydryl groups in myosin adenosine triphosphate. *Biochemistry* **13**, 2014–2022
42. Willner, I., Rubin, S., and Riklin, A. (1990) Photoregulation of papain activity through anchoring photochromic azo groups to the enzyme backbone. *J. Amer. Chem. Soc.* **113**, 3321–3325
43. Willner, I. and Rubin, S. (1996) Control of the structure and functions of biomaterials by light. *Angew. Chem. Int. Ed. Engl.* **35**, 367–385
44. Burke, M. and Reisler, E. (1977) Effect of nucleotide binding on the proximity of the essential sulfhydryl groups of myosin. chemical probing of movement of residues during conformational transitions. *Biochemistry* **16**, 5559–5564
45. Miller, L., Coppedge, J., and Reisler, E. (1982) The reactive SH1 and SH2 cysteines in myosin subfragment 1 are crosslinked at similar rates with reagents of different length. *Biochem. Biophys. Res. Commun.* **106**, 117–122
46. Hiratsuka, T. (1999) ATP-induced opposite changes in the local environments around Cys 697 (SH2) and Cys 707 (SH1) of the myosin motor domain revealed by the prodan fluorescence. *J. Biol. Chem.* **274**, 29156–29163
47. Sugimoto, Y., Okumura, T., Arata, T., Takezawa, Y., and Wakabayashi, K. (2000) An X-ray solution scattering study on the conformation of *p*PDM-crosslinked myosin subfragment-1 trapping MgADP. *Photon Factory Activity Report (KEK)* **18A**, 233
48. Sugimoto, Y., Arata, T., and Wakabayashi K. (2003) Energy tranducing conformation changes of myosin motor domain. *Photon Factory Activity Report (KEK)* **20B**, 42–43